Spectroscopy on magnetically confined plasmas using electron beam ion trap spectrometers[1]

A. T. Graf, S. Brockington, R. Horton, S. Howard, D. Hwang, P. Beiersdorfer, J. Clementson, D. Hill, M. May, H. Mclean, R. Wood, M. Bitter, J. Terry, W.L. Rowan, J. K. Lepson, and L. Delgado-Aparicio

Abstract: Multiple spectrometers originally designed for and used at the University of California Lawrence Livermore National Laboratory's electron beam ion trap have found use at various magnetically confined plasma facilities. Three examples will be described. First is a soft X-ray/EUV grating spectrometer (6–150 Å), which is operating at the National Spherical Torus Experiment. Second is an EUV spectrometer with wavelength coverage up to 400 Å, which has just recently started operating at the Sustained Spheromak Physics Experiment. The last is a high-resolution transmission-grating spectrometer for visible light that has been used at the Compact Toroid Injection Experiment and is currently at the Alcator C-Mod tokamak.

PACS Nos.: 39.30.+w, 52.55.−s, 32.30.Rj, 07.60.Rd, 52.70.La

Résumé : Plusieurs spectromètres initialement conçus pour utilisation au laboratoire du piège ionique à faisceau d'électrons du Lawrence Livermore National Laboratory de l'University of California ont été utilisés à divers laboratoires étudiant le confinement magnétique du plasma. Nous donnons trois exemples. Le premier est un spectromètre à réseau pour rayons-X mous/EUV (6–150 Å), qui est présentement utilisé au National Spherical Torus Experiment. Le deuxième est un spectromètre EUV qui couvre les longueurs d'onde jusqu'à 400 Ået qui a récemment commencé à fonctionner au Sustained Spheromak Physics Experiment. Le dernier est un spectromètre par transmission à réseau de haute résolution pour la lumière visible qui a été utilisé au Compact Toroid Injection Experiment et qui est actuellement au tokamak Alcator C-Mod.

[Traduit par la Rédaction]

1. Introduction

Spectroscopy is a valuable, noninvasive diagnostic for all plasmas. In particular, work done at the University of California's Lawrence Livermore National Laboratory (LLNL) electron beam ion trap (EBIT) facility continues to establish useful benchmarks for atomic physics that can be used to diagnose characteristics of less well understood plasmas. A multitude of spectrometers have been developed and used at the LLNL electron beam ion traps [1–10]. Each are state-of-the-art instruments, many of which can be adapted to diagnosing magnetically confined plasmas. In these new environments they contribute to the science performed by providing data on plasma conditions that are otherwise not available. Three examples with results from four facilities will be described. These include a flat field grazing-incidence reflection-grating spectrometer for soft X-ray and Extreme Ultraviolet (EUV) light used at the National Spherical Torus Experiment (NSTX) [11] and a longer wavelength spectrometer used at the Sustained Spheromak Physics Experiment (SSPX). Finally, a description of a high spectral resolution transmission-grating spectrometer [12] for visible light used at the Compact Toroid Injection Experiment (CTIX) and the Alcator C-Mod tokamak is given. In all instances, the EBIT spectrometers have provided valuable data on plasma performance such that the spectrometers have been integrated into the general diagnostic suites at these facilities and provide data on an ongoing basis.

Received 9 March 2007. Accepted 11 April 2007. Published on the NRC Research Press Web site at http://cjp.nrc.ca/ on 14 February 2008.

A. T. Graf,[2] S. Brockington, R. Horton, S. Howard, and D. Hwang. University of California, Davis, CA 95616, USA.
P. Beiersdorfer, J. Clementson, D. Hill, M. May, H. Mclean, and R. Wood. Lawrence Livermore National Laboratory, Livermore, CA 94550, USA.
M. Bitter. Princeton Plasma Physics Laboratory, P.O. Box 451 Princeton, NJ 08543, USA.
J. Terry. Plasma Science and Fusion Center, MIT, Cambridge, MA 02139, USA.
W.L. Rowan. Fusion Research Center, University of Texas at Austin, Austin, TX 78712, USA.
J. K. Lepson. University of California, Berkeley, CA 94720, USA.
L. Delgado-Aparicio. Johns Hopkins University, Baltimore, MD 21218, USA.

[1]Paper given at the Workshop on Twenty Years of Spectroscopy with EBIT held in Berkeley, California, 13–15 November 2006.
[2]Corresponding author (e-mail: agraf@psfc.mit.edu).

 doi: 10.1139/P07-117 © 2008 NRC Canada

2. Soft X-ray/EUV spectrometer (6–150 Å)

2.1. Experiments at the electron beam ion trap

For some perspective, we give a brief review of the spectroscopic characteristics [1] and some of the results obtained previously at the electron beam ion trap using the soft X-ray grazing-incidence spectrometer. The dispersion element is a variable line spacing concave reflection grating [13, 14], which creates a flat field of focus and allows the use of a two-dimensional array detector such as a Photometrics, cryogenically cooled, back-illuminated charge-coupled device (CCD). The grating has a variable line spacing with on average 2400 lines/mm allowing a resolving power of 300 to 600 at 25 and 50 Å, respectively. The blazing angle is 1.3°. The wavelength coverage is roughly 50 Å/frame anywhere between 6 and 150 Å. Since the electron beam width is ~50 μm, there is no entrance or exit slit. Differential pumping is used between the spectrometer housing (10^{-6} torr) and the EBIT vacuum chamber (10^{-11} torr).

Many experiments have benefited from the use of this spectrometer. Träbert et al. [15] were able to investigate line emission between 20 and 60 Å from Br-like Au^{44+} to Co-like Au^{52+} by systematically increasing the electron beam energy to separate the resulting charge states. Using the Hebrew University Lawrence Livermore Atomic Code [16] it was possible to identify various $\Delta n = 0$ ($n = 4$–4) transitions in Rb-like Au^{42+} to Cu-like Au^{50+} to a higher precision than previous observations on other experiments. In a similar manner, Utter et al. [17] were able to identify roughly 60 features in Rb-like W^{37+} through Cu-like W^{45+} between 40 and 85 Å. Also, Beiersdorfer et al. [18] discovered magnetic-field sensitive Ne-like lines in the EUV and demonstrated this in Ar^{8+} spectra. An external magnetic field allows the mixing of sublevels of neighboring levels with the same magnetic quantum number and parity, possibly permitting an otherwise strictly forbidden transition to occur. If one of the interacting sublevels has a significantly larger radiative decay channel, the intensity of an otherwise dim line will be significantly enhanced. The intensity can be related back to the magnetic field. Other examples can be found in the refs. 1 and 19.

2.2. Experiments at the National Spherical Torus Experiment

The National Spherical Torus Experiment [20] at the Princeton Plasma Physics Laboratory is primarily a facility for determining the feasibility of a near-unity aspect-ratio toroidal magnetic confinement scheme for a fusion reactor. Some of the peak characteristics include an aspect ratio, $R/a \sim 1.3$, a pulse length of ~1 s, a plasma current, $I_p = 1.5$ MA, a toroidal magnetic field, $B_T \leq 0.55$ T, and an electron temperature and density of $T_e \leq 1.2$ keV and $n_e \leq 8 \times 10^{19}$ m^{-3}, respectively, during neutral beam heated discharges.

Some modifications were made to the original spectrometer design to be appropriate for use at NSTX. For example, the plasma source is now extended, requiring an entrance slit (typically between 30 and 100 μm) to preserve spectral resolution. Also, since the discharges are transient (1.5 s) and are dynamic, a mechanical shutter is used to obtain exposures as short as one 50 ms frame per plasma. It is possible to create a fairly repeatable discharge and build up a temporal description of a spectrum by moving the exposure window in time incrementally. The spectrometer has a radial view at the mid-plane, thus allowing the observation of all available charge states of an ion of interest. During neutral beam injection into NSTX plasmas, neutrons are produced, which, in principle, can adversely affect the performance of the CCD camera and contribute to background noise. No noise or pixel failure attributed to neutrons has been seen, although no shielding against neutrons has been employed. However, a background attributed to hard X-rays is seen in the spectrum whenever the neutral beam sources are operated on NSTX. The reason the detected counts are attributed to hard X-rays and not to neutrons is because they are also detected in the absence of plasma, for example, before the NSTX discharge, or during high-voltage (80 kV) conditioning of the neutral beam ion sources. Lead shielding may reduce this background, but has not been implemented because the effect prevents measurements only in extreme cases and because of cost.

Fig. 1. K-shell emission from O and C as well as L-shell emission from Fe from the National Spherical Torus Experiment shot # 114459 using the soft X-ray/EUV spectrometer.

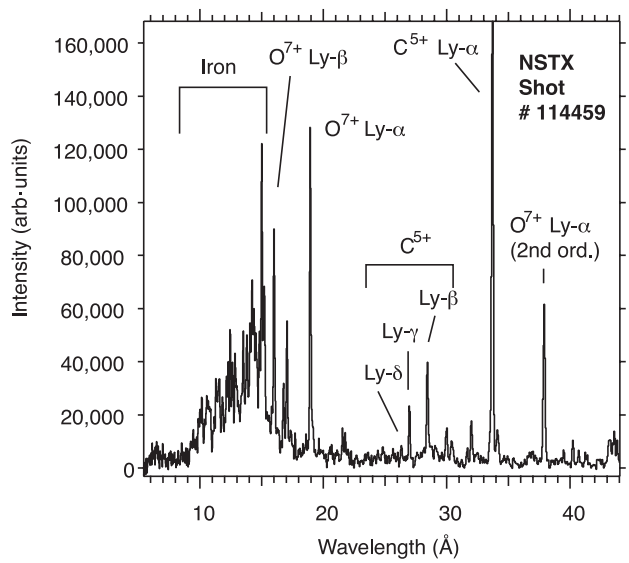

Initial tests of the spectrometer [11] were done by looking at impurities in the plasma between 5 to 65 Å, namely, the K-shell emission from B, O, C, and N as well as L-shell emission from Ar, Fe, and Ni (Fig. 1). Impurity monitoring is important to the NSTX operation for several reasons. The presence of high-Z metal ions indicates erosion of plasma-facing materials. Further, a decrease in boron suggests that the effects of the boronization process may also decrease. Boronization is meant to reduce the amount of high-Z impurities present from the containment vessel structure, allowing a decrease in radiated power and an increase in confinement. Finally, gases are puffed into the plasma for transport studies. An example of a Ne puff is shown in Fig. 2. Two spectra from identical discharges are shown. The neon puff can clearly be seen.

The NSTX plasma is at a higher density than the electron beam ion trap ($n_e = 10^{17}$ m^{-3}) and the energy distribution

© 2008 NRC Canada

Fig. 2. Two overlaid National Spherical Torus Experiment shots obtained using the soft X-ray/EUV spectrometer. The discharges are identical except one had Ne puffed for transport studies.

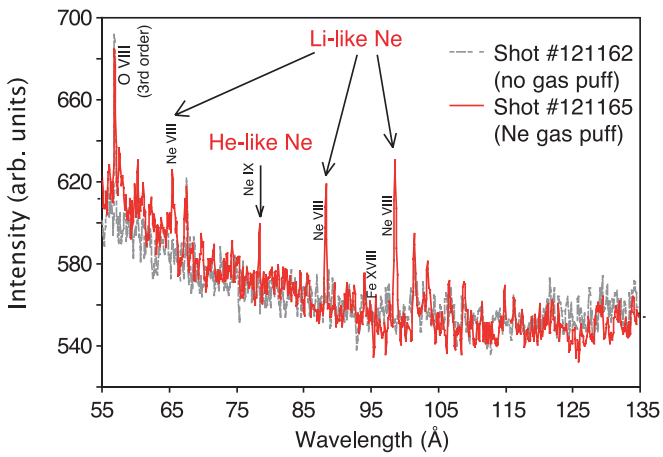

Fig. 3. Time-integrated spectra from four Sustained Spheromak Physics Experiment discharges using the EUV spectrometer. Shown are preliminary identification of some impurity species including O^{4-5+}, N^{4+}, and B^{3+}.

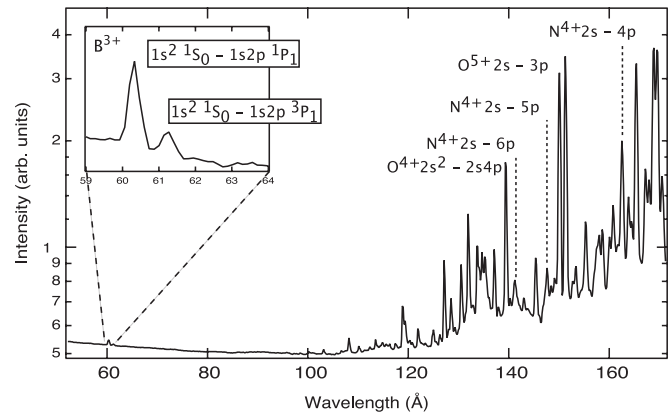

is roughly Maxwellian as opposed to being mono-energetic. These differences along with a well-diagnosed electron temperature from Thomson scattering make possible a spectral line ratio calibration for comparison to astrophysical sources. One measurement in particular has helped to unravel a long-standing debate concerning line ratios between the major $3s \rightarrow 2p$ and $3d \rightarrow 2p$ transitions in Fe XVII around 15 and 17 Å, respectively. The Astrophysical Plasma Emission Code predicts a smaller line ratio than measured from astrophysical sources. It has been suggested that resonant scattering within an optically thick plasma of one of the $3s \rightarrow 2p$ transitions (3C at 15.01 Å) is the culprit [21]. Beiersdorfer et al. [22, 23] have shown that the optically thin tokamak plasmas in DITE, PLT, and JET as well as in NSTX can produce the same line ratio as astrophysical results. This rules out opacity as being necessary for the explanation and directs the attention back to theoretical predictions. Further information can be found in Brown's contribution to these proceedings [24] as well as in ref. 25.

3. EUV spectrometer (25–400 Å)

3.1. Experiments at the electron beam ion trap

This spectrometer is similar to that previously described in Sect. 2. Here, a 1200 lines/mm grating allows a resolving power of more than 300 and 600 at 100 and 200 Å, respectively. The focusing field is flat permitting the use of a two-dimensional array, liquid-nitrogen-cooled, back-illuminated CCD as the detector. It is in fact the same type of detector as described in Sect. 2.1. The CCD has a 1 in range of motion (1 in = 2.54 cm), which makes the coverable wavelength from 25 to 400 Å, with ≤200 Å/frame. The beam again acts as an entrance slit but there are additional slitted apertures to block X-ray light and reduce the gas load on the EBIT chamber.

The first demonstration of this spectrometer showed that it was possible to resolve the forbidden transition $1s^2\,{}^1S_0 \rightarrow 1s2s\,{}^3S_1$ in He-like N^{5+} [10] from the Li-like N^{4+} inner-shell-excited satellite $1s2s2p\,{}^2P_{3/2} \rightarrow 1s^2 2s\,{}^2S_{1/2}$. This allowed a correction to the identification of these lines used as a transport diagnostic in Alcator C-Mod [26]. Beiersdorfer et al. [27], in another experiment, concentrated on EUV emission from Fe VII, Fe VIII, Fe IX, and Fe X and found in addition to a few prominent line features, a multitude of smaller features that creates an underlying continuum that are not included in the MEKAL or CHIANTI data bases. It is pointed out that this incompleteness in spectral flux inclusion could explain the poor results from global-fitting techniques applied to the Extreme-Ultraviolet Explorer satellite data. Finally, by using the low-energy capabilities of EBIT, Lepson et al. [28] extended the experimental data base of spectral lines from Neon-like ions down to Si V, S VII, and Ar IX.

3.2. Experiments at SSPX

The Sustained Spheromak Physics Experiment [29] at LLNL is yet another option being evaluated for use as a magnetic confinement fusion reactor. It differs from a spherical tokamak in that there is no central column and the plasma is created and potentially sustained by way of helicity and particle injection from a Marshall gun. Its peak characteristics include a pulse length of 4 ms, an injector current of 200 kA, and an electron temperature and density of $T_e = 350$ eV and $n_e = 10^{20}$ m^{-3}, respectively.

The spectrometer fielded at SSPX is structured similar to that at NSTX except it uses the 1200 lines/mm grating as described in Sect. 3.1. Since the plasma duration is relatively short, a mechanical shutter is useless and the entire 2–4 ms discharge is time integrated. The view is roughly 1 m from the plasma directed at the mid-plane with a slight toroidal tilt. Preliminary results before the onset of SSPX upgrades have allowed some of the impurities to be identified including emission from O^{4-5+}, N^{4+}, and B^{3+} (Fig. 3).

4. Transmission grating spectrometer (3600–6700 Å)

4.1. Experiments at the electron beam ion trap

Again, for perspective, the characteristics of the transmission grating spectrometer [3] and some of its uses at the electron beam ion trap are described in the following. The diffrac-

© 2008 NRC Canada

tion element is a 6 in diameter transmission grating with 2857 lines/mm. An instrument spectral line width has been demonstrated to be as small as 0.4 Å (at 5676 Å). The diameter of the grating along with comparably large but with small focal-length focusing optics allows a high optical throughput (for example, $f/\# = 3.1$). The detector is a two-dimensional Photometrics cryogenically cooled, back-illuminated CCD as in Sects. 2.1 and 3.1. This detector permits a 130 Å bandwidth anywhere within 3600 to 6700 Å. The electron beam width, again acts as a pseudo entrance slit.

The high spectral resolution of this spectrometer allowed Beiersdorfer et al. [30] to resolve the hyperfine splitting of the $1s$ state between two H-like $^{205}Tl^{80+}$ and $^{203}Tl^{80+}$ isotopes. This gave a higher precision measurement of the nuclear magnetization radii (the results being 5.89(14) and 5.83(14) fm, respectively). Chen et al. [31] made a methodic study of visible Kr emission appropriate for radiative cooling in the edge of magnetic confinement devices. A total of 78 features were identified existing in neutral to He-like Kr^{34+}. Other examples of work done at the electron beam ion trap with this spectrometer can be found in refs. 32–34.

4.2. Experiments at CTIX

The design of the Compact Toroid Injection Experiment [35] is based on a Marshall gun whose original purpose is to fuel tokamak plasmas. The gun is a coaxial arrangement that creates and accelerates a small (i.e., 5–50 μg) spheromak plasma up to 200 km/s. Some peak characteristics of the plasma include a shot duration of 60 μs, a repetition rate of 0.05 Hz (1 shot every 20 s), and an electron temperature and density of $T_e = T_i \leq$ 50 eV and $n_e = 10^{21}$ m^{-3}, respectively. Various gases can be used such as H, He, and Ar.

Some alterations of the original design of the spectrometer were necessary to be useful in diagnosing the CTIX plasma. The short duration of a discharge required using a two-dimensional DiCam Pro gated intensified CCD from Cooke. The camera allowed a single 1 μs exposure per discharge. The reproducibility and fast repetition rate of CTIX were key to obtaining time-resolved spectra. Four spatially localized, simultaneous views were possible using fiber optics vertically separated at the entrance slit. Three were placed at various ports along the length of the gun with transverse views of the plasma and one view down the barrel. This was ideal for measuring ion velocity from Doppler shifts since line emission from the latter view should be blue-shifted with respect to the other three.

An impurity survey was recorded which produced a rich region of line emission from He^{1+}, O^{1+}, and N^{1+} that could be captured in the bandwidth of a single shot. Performing multiple 1 μs exposures propagated in time from shot to shot allowed a temporally resolved spectrum for line-integrated Doppler-velocity measurements [12]. The first 19 μs of data is shown again here for completeness in Fig. 4. There are two peculiar features to the result. First, the velocity of the He^{1+} peaks twice. The first peak is the expected qualitative acceleration of the compact torus while the second is coincident in time with a restrike that results from electrical ringing of the injector circuit. The second curiosity is that the He^{1+} peaks to only 70 km/s upon leaving the end of the accelerator. This disagrees with

Fig. 4. Line-integrated impurity Doppler-velocity measurements in the Compact Toroid Injection Experiment for the the first 19 μs of discharge for He^{1+}, O^{1+}, and N^{2+} using the transmission grating spectrometer [12].

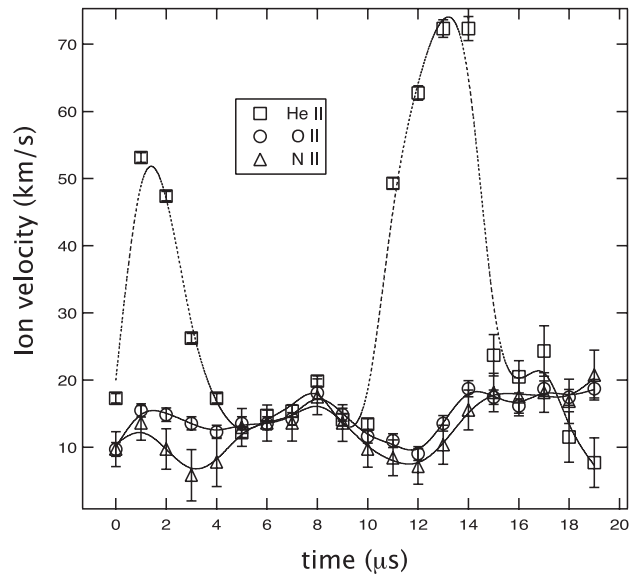

magnetic probe measurements that suggest a peak velocity of 200 km/s. A possible explanation for the discrepancy is that the He^{1+} becomes bare He and thus ceases to radiate before it is fully accelerated. An electron temperature of 54.4 eV is sufficient to do this. Further, photodiodes filtered for ±20 Å around the brightest He^{1+} emission line (at 4685.5 Å) and displaced along the length of the gun show a clear decrease in the peak signal as the plasma propagates. One further observation is that the heavier impurities tend to drag behind the lighter ones, which is desirable if a compact toroid injector is to be used for tokamak fueling. In a separate experiment, an attempt was made to measure toroidal rotation velocity of the compact toroid by using opposing transverse views. No rotation was seen for integration times of 1 μs though recent magnetic measurements along with Lagrangian interpolation methods [36] suggest a velocity reversal from front to back of the torus. To see this would require integration times on the order of 0.1 μs for the spectrometer. The order of magnitude of the toroidal velocity is thought to be comparable to the bulk velocity (i.e., as much as 200 km/s).

4.3. Experiments at Alcator C-Mod

The Alcator C-Mod tokamak [37] at the Plasma Science and Fusion Center at MIT, is a compact high-magnetic-field experimental fusion device. It operates with an aspect ratio, $R/a = 3.2$, toroidal magnetic field, $B_T = 6$–8 T, a pulse length of 4 s, a plasma current, $I_p = 1.5$ MA, and a peak electron temperature and density of $T_e = T_i = 2 - 3$ keV and $n_e = 10^{21}$ m^{-3}, respectively.

Alcator C-Mod produces a dynamic transient plasma requiring high (~1 ms) time resolution. The use of a Hamamatsu linear photodiode array for detection yielded unsatisfactory results. The arrays sensitivity was much less than expected and produced poor signal-to-noise for the measured spectra. The

© 2008 NRC Canada

Fig. 5. Partial visible survey in Alcator C-Mod using the transmission grating spectrometer. The well-known features include the deuterium Balmer series (top), and emission lines from F^{1+}, He^{1+}, Cl^{1+}, and B^{1+} and B^{4+} at 4940.38 and 4944.67 Å, respectively. The identification of the remaining features is still preliminary.

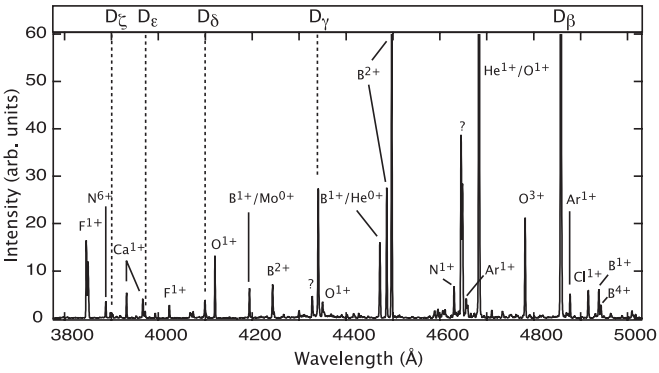

present detector is a low read noise camera as described in Sect. 2.1. The signal-to-noise is much improved. Unfortunately, what one gains in a decreased readout noise one also loses in the readout rate (for example, 1 frame/min). Time resolution is achieved by moving the camera vertically through the dispersion plane during a discharge, as described in ref. 12. This allows spectral measurements on the order of 100 Hz. This approach restricts the number of spatial views to 1.

The Alcator C-Mod plasma is ideal for investigating the radial distribution of intrinsic toroidal and poloidal rotation in regimes appropriate to ITER-type operating scenarios. In contrast to most tokamaks, the primary heating mechanism in C-Mod is from ion cyclotron and lower hybrid resonant-frequency antennas. This is significant in that the antennas impart no direct momentum or particle input to the plasma. This would otherwise complicate the analysis of Doppler-velocity and temperature measurements. The core-ion velocity is diagnosed using Doppler shifts of X-ray line emission while visible spectroscopy is used in the region around the last closed flux surface. Between the two, UV spectroscopy or possibly visible emission from magnetic dipole transitions of higher Z impurities such as Ar or Kr (for example, $2s^2 2p\,^2P_{1/2} \rightarrow {}^2P_{3/2}$ in Al-like Ar^{13+} at 4413 Å and $3s^2 3p^2\,^3P_1 \rightarrow {}^3P_2$ in Si-like Kr^{22+} at 3841.1 Å) is appropriate. This requires a light-sensitive high optical throughput device such as our spectrometer. A visible survey was conducted to identify impurities that may be useful for probing different spatial locations in the plasma (Fig. 5). Multiple impurities including B^{1+}, B^{2+}, B^{4+}, O^{1+}, and Cl^{1+} were identified. Examples of impurity ion velocity measurements at various locations are seen Figs. 6*a* and 7*a*. Doppler-velocity measurements using active charge exchange between neutral deuterium from either a gas puff or a radially oriented diagnostic beam and the deuterium majority species are also being performed. A direct comparison of velocity profiles from impurity and majority species is vital to understanding plasma rotation in tokamaks.

Fig. 6. Alcator C-Mod shot 1060314012: The top two plots reflect data taken with the transmission grating spectrometer using an inner-wall toroidal view. (*a*) Line-integrated Doppler-velocity measurements using emission from D_β and the $2s3d\,^1D_2 \rightarrow 2s3d\,^1F_2$ transition from B^{1+} (see Fig. 5) in units of km/s. (*b*) Corresponding signal level in units of 10^3 counts. (*c*) D_α emissivity. (*d*) Line-integrated electron density in units of 10^{18} cm^{-3}. (*e*) Net power input from all the Ion Cyclotron Resonance Frequency antennas in units of MW.

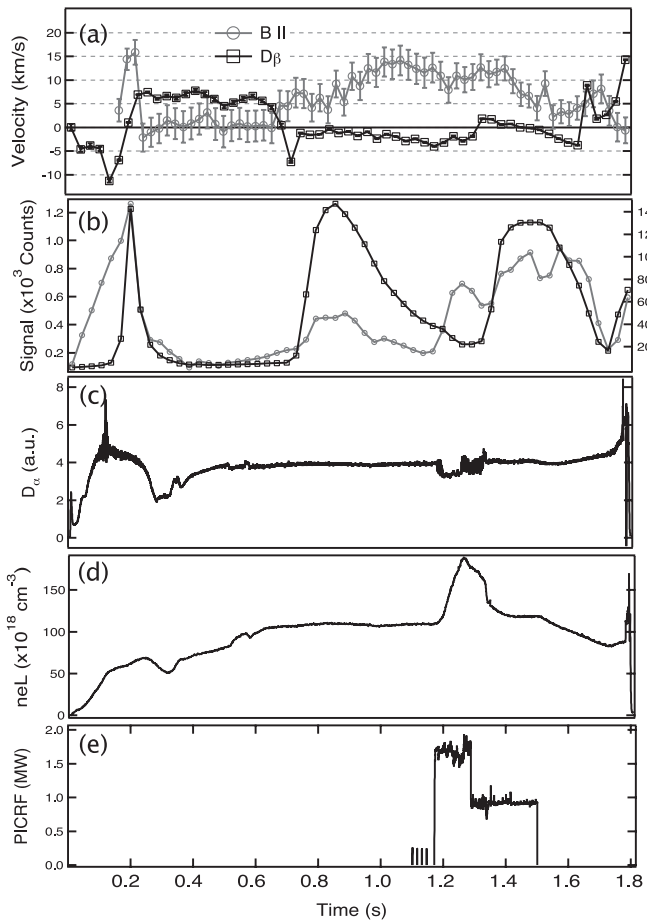

5. Summary

Multiple spectrometers originally designed for and successfully used at the University of California Lawrence Livermore National Laboratory's electron beam ion traps have been very productive as diagnostics for other magnetically confined plasmas. Several examples are given here and compared with the spectrometers original use at the LLNL EBIT's. First, is a soft X-ray/EUV grating spectrometer (6–150 Å), which is operating at the National Spherical Torus Experiment. This spectrometer has allowed intrinsic and puffed impurity identification and monitoring of emission from K-shell B, O, C, and N as well as L-shell emission from Ar, Fe, Ni, and Ne between 5 and 135 Å. Also, the investigation of commonly used and controversial L-shell Fe emission line ratio diagnostics for comparison to results from EBIT and celestial sources has helped to redirect the attention back to the improvement of theoretical results. Second, is an EUV spectrometer with wavelength cov-

© 2008 NRC Canada

Fig. 7. Alcator C-Mod shot 1060616006: The top two plots reflect data taken with the transmission grating spectrometer using a poloidal view at $R = 0.9$ m (i.e, ~2 cm outside the last closed flux surface. (*a*) Line integrated Doppler-velocity measurements from two separate B^{2+} lines at ~4487 and 4497 Å and from a blend of O^{1+} and neutral He^{1+} at 4686 Å, in units of km/s. Refer to Fig. 5. (*b*) Corresponding signal level in units of 10^3 counts. (*c*) D_α emissivity. (*d*) Line-integrated electron density in units of 10^{18} cm^{-3}. (*e*) Net power input from all the Ion Cyclotron Resonant Frequency antennas in units of MW.

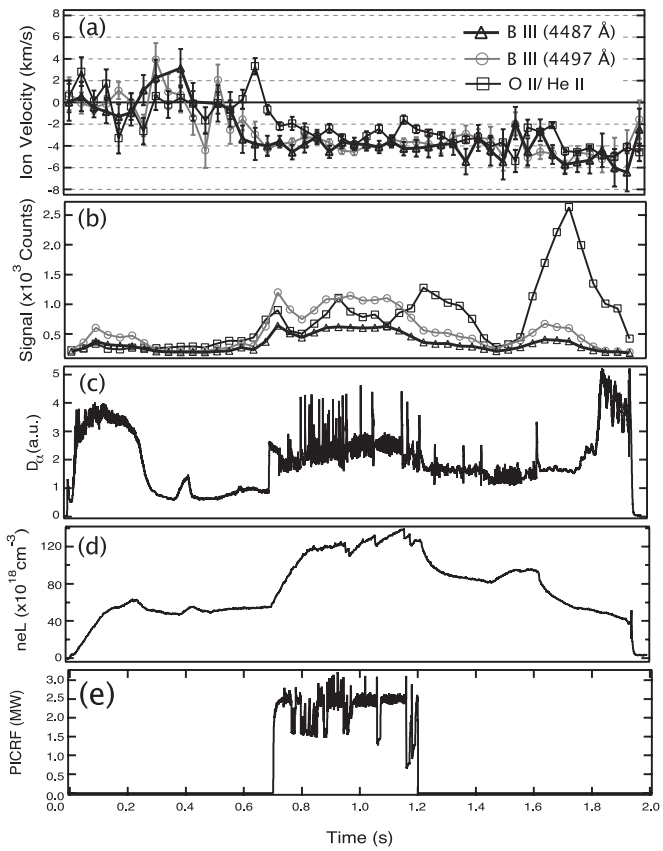

erage up to 400 Å, which has just recently started operating at the Sustained Spheromak Physics Experiment. First results have allowed preliminary identification of intrinsic impurities including emission lines from O^{4-5+}, N^{4+}, and B^{3+}. Finally, is a high-resolution transmission-grating spectrometer for visible light (3600–6700 Å) that has been used at the Compact Toroid Injection Experiment and is currently at the Alcator C-Mod tokamak. Results from CTIX have yielded an impurity survey and time-resolved line-integrated impurity Doppler-velocity measurements. The work at Alcator C-Mod has also yielded an impurity survey as well as both toroidal and poloidal line-integrated Doppler measurements of various impurities as well as the majority species.

All of the spectrometers mentioned continue to be of use at the respective facilities. In fact, additional instrumentation has been added at various facilities. For example, the EBIT 1 m normal-incident grating spectrometer [38] has been implemented at CTIX as an impurity monitor. Spectrometers from the Livermore EBIT facility thus continue to answer important questions in plasma research not only by improving the state of knowledge of atomic physics and atomic spectroscopy through experiments conducted on EBIT itself, but also by direct observation of the plasmas of interest at remote locations. Needless to say that by doing so, also valuable feedback is generated, which, for example, allows tailoring of atomic physics experiments on EBIT to the needs at magnetic fusion devices.

Acknowledgements

This work was performed under the auspices of the US Department of Energy by UC-LLNL, under contracts W-7405-Eng-48, DE-FGO2-O3ER54732, and DE-FGO3-96ER54373 and by PPPL under contract DE-AC02-76CHO3073.

References

1. S.B. Utter, G.V. Brown, P. Beiersdorfer, E.J. Clothiaux, and N.K. Podder. Rev. Sci. Instrum. **70**, 284 (1999).
2. S.B. Utter, P. Beiersdorfer, and G.V. Brown. Phys. Rev. A, **61**, 030503 (2000).
3. S.B. Utter, J. R. Crespo López-Urrutia, P. Beiersdorfer, and E. Träbert. Rev. Sci. Instrum. **73**, 3737 (2002).
4. P. Beiersdorfer and B.J. Wargelin. Rev. Sci. Instrum. **65**, 13 (1994).
5. P. Beiersdorfer, J.R. Crespo López-Urrutia, E. Förster, J. Mahiri, and K. Widman. Rev. Sci. Instrum. **68**, 1077 (1997).
6. G.V. Brown, P. Beiersdorfer, and K. Widman. Rev. Sci. Instrum. **70**, 280 (1999).
7. P. Beiersdorfer, E.W. Magee, E. Träbert, H. Chen, J.K. Lepson, M.-F. Gu, and M. Schmidt. Rev. Sci. Instrum. **75**, 3723 (2004).
8. B.K.F. Young, A.L. Osterheld, D.F. Price, R. Shepherd, R.E. Stewart, A.Ya. Faenov, A.I. Magunov, T.A. Pikuz, I.Yu. Skobelev, F. Flora, S. Bollanti, P. Di Lazzaro, T. Letardi, A. Grilli, L. Palladina, A. Reale, A. Scafati, and L. Reale. Rev. Sci. Instrum. **69**, 4049 (1998).
9. N. Nakamura, E. Nojikawa, H. Shiraishi, F.J. Currell, S. Ohtani, A.Ya. Faenov, and T.A. Pikuz. Rev. Sci. Instrum. **70**, 1658 (1999).
10. P. Beiersdorfer, J.R. Crespo López-Urrutia, P. Springer, S.B. Utter, and K.L. Wong. Rev. Sci. Instrum. **70**, 276 (1999).
11. P. Beiersdorfer, M. Bitter, L. Roquemore, J.K. Lepson, and M.-F. Gu. Rev. Sci. Instrum. **77**, 10F306 (2006).
12. A.T. Graf, S. Howard, R. Horton, D. Hwang, M. May, P. Beiersdorfer, and J. Terry. Rev. Sci. Instrum. **77**, 1 (2006).
13. T. Harada and T. Kita. Appl. Opt. **19**, 3987 (1980).
14. N. Nakano, H. Kuroda, T. Kita, and T. Harada. Appl. Opt. **23**, 2386 (1984).
15. E. Träbert, P. Beiersdorfer, K.B. Fournier, S.B. Utter, and K.L. Wong. Can. J. Phys. **79**, 153, (2001).
16. A. Bar-Shalom, M. Klapisch, and J. Oreg. J. Quant. Spectrosc. Rad. Trans. **71**, 169 (2001).
17. H. Chen, P. Beiersdorfer, K.B. Fournier, and E. Träbert. Phys. Rev. E, **65**, 056401 (2002).
18. P. Beiersdorfer, J.H. Scofield, and A.L. Osterheld. Phys. Rev. Lett. **90**, 23, 235003 (2003).
19. S.B. Utter, P. Beiersdorfer, and E. Träbert. Can. J. Phys. **80**, 1503 (2002).

© 2008 NRC Canada

20. M. Ono, S.M. Kaye, Y.-K.M. Peng, G. Barnes, W. Blanchard, M.D. Carter, J. Chrzanowski, L. Dudek, R. Ewig, D. Gates, R.E. Hatcher, T. Jarboe, S.C. Jardin, D. Johnson, R. Kaita, M. Kalish, C.E. Kessel, H.W. Kugel, R. Maingi, R. Majeski, J. Manickam, B. McCormack, J. Menard, D. Mueller, B.A. Nelson, B.E. Nelson, C. Neumeyer, G. Oliaro, F. Paoletti, R. Parsells, E. Perry, N. Pomphrey, S. Ramakrishnan, R. Raman, G. Rewoldt, J. Robinson, A.L. Roquemore, P. Ryan, S. Sabbagh, D. Swain, E.J. Synakowski, M. Viola, M. Williams, J.R. Wilson, and the NSTX team. Nucl. Fusion, **40**, 557 (2000).
21. H.R. Rugge and D.L. McKenzie. Astrophys. J. **297**, 338 (1985).
22. P. Beiersdorfer, M. Bitter, S. von Goeler, and K.W. Hill. Astrophys. J. **610**, 616 (2004).
23. P. Beiersdorfer, M. Bitter, S. von Goeler, and K.W. Hill. *In* X-ray Diagnostics of Astrophysical Plasmas. *Edited by* R.K. Smith. AIP Conf. Proc. No 774. AIP, Melville, New York. 2005. p. 83–91.
24. G.V. Brown. Can. J. Phys. **86** (2008). This issue.
25. G.V. Brown, P. Beiersdorfer, H. Chen, J.H. Scofield, K.R. Boyce, R.L. Kelley, C.A. Kilbourne, F.S. Porter, M.F. Gu, S.M. Kahn, and A.E. Szymkowiak. Phys. Rev. Lett. **96**, 253201 (2006).
26. J. Rice, J.L. Terry, J.A. Goetz, Y. Wang, E.S. Marmar, M. Greenwald, I. Hutchinson, Y. Takase, S. Wolfe, H. Ohkawa, and A. Hubbard. Phys. Plasmas, **4**, 1605 (1997).
27. P. Beiersdorfer, J.K. Lepson, G.V. Brown, S.B. Utter, S.M. Kahn, D.A. Liedahl, and C.W. Mauche. Astphys. J. **519**, L185 (1999).
28. J.K. Lepson and P. Beiersdorfer. Phys. Scr. **T120**, 62 (2005).
29. E.B. Hooper, L.D. Pearlstein, and R.H. Bulmer. Nucl. Fusion, **39**, 863 (1999).
30. P. Beiersdorfer, S.B. Utter, K.L. Wong, J.R. Crespo López-Urrutia, J.A. Britten, H. Chen, C.L. Harris, R.S. Thoe, D.B. Thorn, E. Träbert, M.G.H. Gustavsson, C. Forssén, and A. Mårtensson-Pendrill. Phys. Rev. A, **64**, 032506 (2001).
31. H. Chen, P. Beiersdorfer, C.L. Harris, and S.B. Utter. Phys. Scr. **66**, 133 (2002).
32. E. Träbert, S.B. Utter, and P. Beiersdorfer. Phys. Lett. **272A**, 86 (2000).
33. H. Chen, P. Beiersdorfer, C.L. Harris, S.B. Utter, and K.L. Wong. Rev. Sci. Instrum. **72**, 983 (2001).
34. S.B. Utter, P. Beiersdorfer, and E. Träbert. Phys. Rev. A, **67**, 012508 (2003).
35. H.S. Mclean, D.Q. Hwang, R.D. Horton, R.W. Evans, and S.D. Terry. Fusion Tech. **33**, 252 (1998).
36. S.J. Howard, D.Q. Hwang, R.D. Horton, R.W. Evans, S.J. Brockington, and J. Johnson. Method of reconstructing a moving pulse. http://arxiv.org/abs/physics/0702187
37. I.H. Hutchinson, R. Boivin, F. Bombarda, P. Bonoli, S. Fairfax, C. Fiore, J. Goetz, S. Golovato, R. Granetz, M. Greenwald, S. Horne, A. Hubbard, J. Irby, B. LaBombard, B. Lipschultz, E. Marmar, G. McCracken, M. Porkolab, J. Rice, J. Snipes, Y. Takase, J. Terry, S. Wolfe, C. Christensen, D. Garnier, M. Graf, T. Hsu, T. Luke, M. May, A. Niemczewski, G. Tinios, J. Schachter, and J. Urbahn. Phys. Plasmas, **1**, 5, 1511 (1994).
38. S.B. Utter, P. Beiersdorfer, J.R. Crespo López-Urrutia, and E. Träbert. Rev. Sci. Instrum. **70**, 288 (1999).

© 2008 NRC Canada